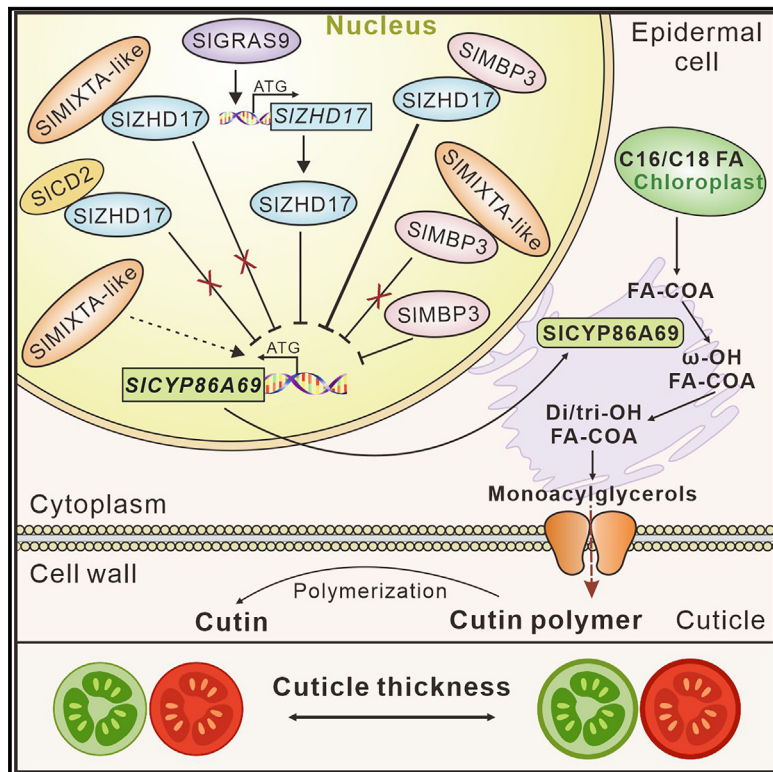


Cutin formation in tomato is controlled by a multipartite module of synergistic and antagonistic transcription factors

Graphical abstract



Authors

Yuan Shi, Changhao Deng, Xiangyin Lu, ..., Yudong Liu, Zhengguo Li, Baowen Huang

Correspondence

bouzayen@ensat.fr (M.B.), yudongliu@cqu.edu.cn (Y.L.), zhengguoli@cqu.edu.cn (Z.L.), huangbaowen2022@cqu.edu (B.H.)

In brief

Shi et al. uncovered the role of SIGRAS9, SIZHD17, and SIMBP3 transcription factors in regulating cutin formation via both synergistic and antagonistic modes. Unveiling the role of this multipartite transcription factor module in cutin biosynthesis defines the cuticle as a novel breeding target for improving postharvest qualities of fleshy fruits.

Highlights

- Cuticle contributes to plant protection against stresses and to fruit postharvest quality
- SIGRAS9, SIZHD17, and SIMBP3 transcription factors coordinately regulate cutin formation
- Cuticle regulators provide breeding targets for improved tolerance to postharvest infections



Article

Cutin formation in tomato is controlled by a multipartite module of synergistic and antagonistic transcription factors

Yuan Shi,^{1,2} Changhao Deng,^{1,2} Xiangyin Lu,^{1,2} Yan Wang,^{1,2} Yaowen Pan,^{1,2} Deding Su,^{1,2} Wang Lu,^{1,2} Yuxiang Lin,^{1,2} Rui Li,^{1,2} Junnan Han,^{1,2} Yanwei Hao,³ Yi Chen,⁴ Ghassen Abid,⁵ Julien Pirrello,⁶ Mondher Bouzayen,^{2,6,*} Yudong Liu,^{7,*} Zhengguo Li,^{1,2,*} and Baowen Huang^{1,2,8,*}

¹Key Laboratory of Plant Hormones Regulation and Molecular Breeding of Chongqing, School of Life Sciences, Chongqing University, Chongqing 401331, China

²Center of Plant Functional Genomics and Synthetic Biology, Institute of Advanced Interdisciplinary Studies, Chongqing University, Chongqing 401331, China

³College of Horticulture, South China Agricultural University, Guangzhou 510642, China

⁴Zhejiang Key Laboratory of Intelligent Food Logistic and Processing, State Key Laboratory for Managing Biotic and Chemical Threats to the Quality and Safety of Agro-products, Zhejiang-Malaysia Joint Research Laboratory for Agricultural Product Processing and Nutrition, College of Food Science and Engineering, Ningbo University, Ningbo 315800, China

⁵Centre of Biotechnology of Borj-Cedria, Laboratory of Legumes and Sustainable Agrosystems, P.B. 901, Hammam-Lif 2050, Tunisia

⁶Laboratoire de Recherche en Sciences Végétales - Génomique et Biotechnologie des Fruits - UMR5546, Toulouse-INP, CNRS, UPS, Université de Toulouse, Toulouse, France

⁷School of Agricultural Sciences, Zhengzhou University, Zhengzhou 450001, China

⁸Lead contact

*Correspondence: bouzayen@ensat.fr (M.B.), yudongliu@cqu.edu.cn (Y.L.), zhengguoli@cqu.edu.cn (Z.L.), huangbaowen2022@cqu.edu (B.H.)

<https://doi.org/10.1016/j.celrep.2025.115258>

SUMMARY

Cuticles protect plants from water loss and pathogen attack. We address here the functional significance of SIGRAS9, SIZHD17, and SIMBP3 in regulating cutin formation in tomato fruit. The study unveils the role of the multipartite “SIGRAS9-SIZHD17-SIMBP3-SIMIXTA-like” transcription factor module in cutin biosynthesis. Plants deficient in SIGRAS9, SIZHD17, or SIMBP3 exhibit thickened cuticles and a higher accumulation of cutin monomers, conferring extended fruit shelf life and higher tolerance to postharvest fungal infection. SIGRAS9 regulation of cutin is mediated by SIZHD17, a negative regulator of S/CYP86A69. SIZHD17 acts synergistically with SIMBP3 to repress S/CYP86A69, and its interaction with SIMIXTA-like prevents the binding to the S/CYP86A69 promoter, thereby releasing the repression of cutin biosynthesis. SIZHD17 and SIMBP3 synergistically repress cutin biosynthesis, while SIMIXTA-like and SICD2 act antagonistically to SIZHD17 and SIMBP3 on this metabolic pathway. The study defines targets for breeding strategies aimed at improving cuticle-associated traits in tomato and potentially other crops.

INTRODUCTION

Tomato (*Solanum lycopersicum*) is one of the most important vegetables worldwide, not only for fresh eating but also for processed products, due to its richness in nutrients recommended for a healthy diet.^{1,2} As with many other fleshy fruits, tomato is prone to rapid deterioration during postharvest storage. Because of its extreme softening at the ripe stage, tomato fruits are vulnerable to pathogens and mechanical stress during shipping and commercialization.^{3–6} Postharvest decay of fleshy fruit is a major issue, and, so far, the most efficient way to extend tomato shelf life has been through the introgression into commercial varieties of ripening mutant loci such as *ripening inhibitor* (*rin*), *non-ripening* (*nor*), and *never ripe* (*Nr*).^{7–10} However, despite their indisputable effectiveness in extending postharvest shelf

life, these strategies are always at the expense of fruit sensory quality.^{8–13} Delayed or incomplete ripening inevitably results in the suboptimal activation of several metabolic pathways, leading to losses of compounds contributing to essential flavor traits that are characteristic of fully ripe fruit.^{8–13} Therefore, a major challenge for modern tomato breeding is to design novel strategies aimed at reducing excessive softening without affecting the whole ripening process, thereby improving postharvest storability while preserving fruit quality.

Fruit firmness is a complex trait closely linked to the structure and composition of cell wall, intercellular adhesion, and cuticle properties.^{14,15} Most ripening-related textural changes of the pericarp emphasize the important role of cell wall metabolism in controlling fruit softening. However, to what extent the cuticle contributes to maintaining the postharvest quality of tomato fruit



is largely overlooked.^{14,16,17} As an important protective barrier and physical support, the composition and properties of the cuticle impact the development, ripening, and postharvest behavior of fruit by affecting brightness, cracking, shelf life, and resistance to pathogens.^{5,18–23} For example, the *delayed fruit deterioration* (*dfd*) tomato mutant, altered in the allelic variant of the *NOR* gene, displays normal softening.^{19,24–26} However, *dfd* fruits exhibited an extended shelf life and strong resistance to postharvest pathogens, which is considered to be closely related to the composition and properties of the cuticle of *dfd* fruit.^{19,24–26}

The outer epidermal layer of tomato fruit is covered by a thick, protective cuticle that is easy to separate, making this fruit species one of the favorite models for studying the formation and properties of the cuticle.^{27–30} In tomato, cutin accounts for more than 90% of the cuticle and is the key factor determining the thickness and biomechanical properties of the fruit cuticle.^{31,32} Mutation in a single structural gene located upstream of the cutin/wax biosynthesis pathway leads to significant changes in the cuticle structure of tomato fruit.^{33–36} For instance, knockout of the glycerol-3-phosphate acyltransferase gene *S/GPAT6* or the cytochrome P450-dependent fatty acid oxidase gene *S/CYP86A69* leads to dramatic alterations of the fruit cuticle regarding its thickness, composition, and properties.^{37–41} Also, silencing the *S/GDSL1* gene, encoding an extracellular lipase protein localized in the cuticle matrix, reduces cutin deposition in tomato fruit in a dose-dependent manner.^{42,43} Deficiency of a β-ketoacyl-coenzyme A synthase *LeCER6* in tomato results in a significant decrease in the proportion of long-chain n-alkanes in the pericarp and a marked increase in fruit water permeance.⁴⁴ In the last decade, important regulators of cuticle formation in tomato fruit have been characterized, including *SISHIN3*, *SIMIXTA*-like, *SICD2*, *SITAGL1*, *SINOR-like1*, *SIWoolly*, *SIMYB31*, and *SIMYB72*.^{31,38,45–50} Silencing of *SISHIN3* or *SIMIXTA*-like leads to reduced cutin content, a shortened shelf life, and decreased resistance to postharvest pathogens.^{38,46,47} Moreover, *sticky peel* (*pe*), a new allelic variant of *CUTIN DEFICIENT 2* (*CD2*), has a glossy fruit surface, considered to be closely related to cutin deficiency.^{47,48,51} Overexpression of *SITAGL1* in tomato significantly thickens the cuticle, while silencing *SITAGL1* leads to significant changes in epidermal cell structure.⁴⁵ Knockout of *S/NOR-like1* resulted in a micro-cracking phenotype, decreased cutin deposition, and increased wax accumulation.³¹ Furthermore, *SIWoolly* interacts with *SIMYB31* to regulate the expression of *SiCER6*, thereby affecting the wax biosynthesis of tomato fruits.⁴⁹ *SIMYB72* interacts with *SITAGL1* to synergistically regulate the expression of *SIMAH1*, which affects wax accumulation in tomato fruits, thereby affecting the postharvest water loss and susceptibility to *Botrytis cinerea*.⁵⁰

In the present study, we used the tomato as a model system to further dissect the regulatory mechanisms of cuticle formation in a fleshy-type fruit. We show that besides the known transcription factors (TFs) *SISHIN3*, *SIMIXTA*-like, *SICD2*, *SITAGL1*, and *SINOR-like1*, three additional TFs, *SIGRAS9*, *SIZHD17*, and *SIMBP3*, are active regulators of cutin formation and therefore impact the postharvest behavior of tomato fruit. Impaired expression of *SIGRAS9*, *SIZHD17*, or *SIMBP3* not only increases

fruit cuticle thickness and the accumulation of cutin monomers but also extends fruit shelf life and confers fruit tolerance to *Botrytis cinerea*. Our data provide a body of molecular and genetic evidence supporting the view that *SIGRAS9* and *SIZHD17* synergistically regulate cutin formation in tomato fruit. In addition, we show that *SIZHD17*, *SIMBP3*, and *SIMIXTA*-like co-regulate the expression of the cutin key biosynthesis gene *S/CYP86A69* in both an antagonistic and synergistic manner through protein-protein interactions. This study demonstrates that the *SIGRAS9*-*SIZHD17*-*SIMBP3*-*SIMIXTA*-like regulatory module is a major player in the transcription control of cutin biosynthesis and thus constitutes an important determinant of the postharvest storability of tomato fruit.

RESULTS

***SIGRAS9* exhibits high expression level in fruit outer epidermis**

Assessing the content of major cutin monomers at different stages of tomato fruit development indicated that several cutin monomers, including p-coumaric, 16-hydroxy-hexadecanoic acid, and 10,16-dihydroxy-hexadecanoic acid, follow a similar trend, peaking 3 days post-breaker (Br+3) (Figure S1A). Cutin formation consists of multiple enzymatic steps relying on a substantial transcriptomic regulation mediated by cutin-related TFs. To identify potential new regulators of cutin formation, we mined the Tomato Expression Atlas (TEA: <https://tea.solgenomics.net/>) database to investigate the expression patterns of putative TF genes in fruit outer epidermis tissues. Among 1,845 genes annotated as TFs in the tomato genome, 100 are predominantly expressed in the outer epidermis (Figure S1B; Data S1), including *S/TAGL1* and *S/CD2*, known already as important regulators of cuticle development.^{45,48} Notably, a member of the GRAS (derived from GAI, RGA, and SCR) TF family, *S/GRAS9*, exhibited high expression in the fruit outer epidermis and an expression pattern paralleling that of cutin accumulation, thus suggesting its involvement in the regulation of cutin biosynthesis (Figure S1B). Further investigation of *S/GRAS9* expression by quantitative real-time polymerase chain reaction (real-time qPCR) indicated that *S/GRAS9* gene is highly expressed in pericarp and outer epidermis tissues, with the highest transcript levels occurring at the Br+3 stage (Figures S1C and S1D).

***SIGRAS9* loss of function results in altered cuticle formation in tomato fruit**

Using a CRISPR-Cas9 strategy, two independent homozygous *SIGRAS9* knockout lines (*Slgras9*-CR #1 and *Slgras9*-CR #2) were selected in T3 generation. Two *S/GRAS9* knockdown lines (*SIGRAS9*-RNAi #2 and *SIGRAS9*-RNAi #8) were also obtained by an RNAi strategy. Examining the pericarp structure following oil red staining revealed a substantially increased cuticle deposition in *Slgras9*-CR fruit leading to thicker cuticles than in the wild type (WT) throughout fruit ripening stages (Figures 1A and 1B). The enhanced thickness of the cuticle in *Slgras9*-CR fruit was further confirmed by laser scanning confocal microscopy, scanning electron microscopy (SEM), and transmission electron microscopy (TEM) observations of the pericarp tissues (Figures 1A, S2A, and S2B). Moreover, the thick cuticle above

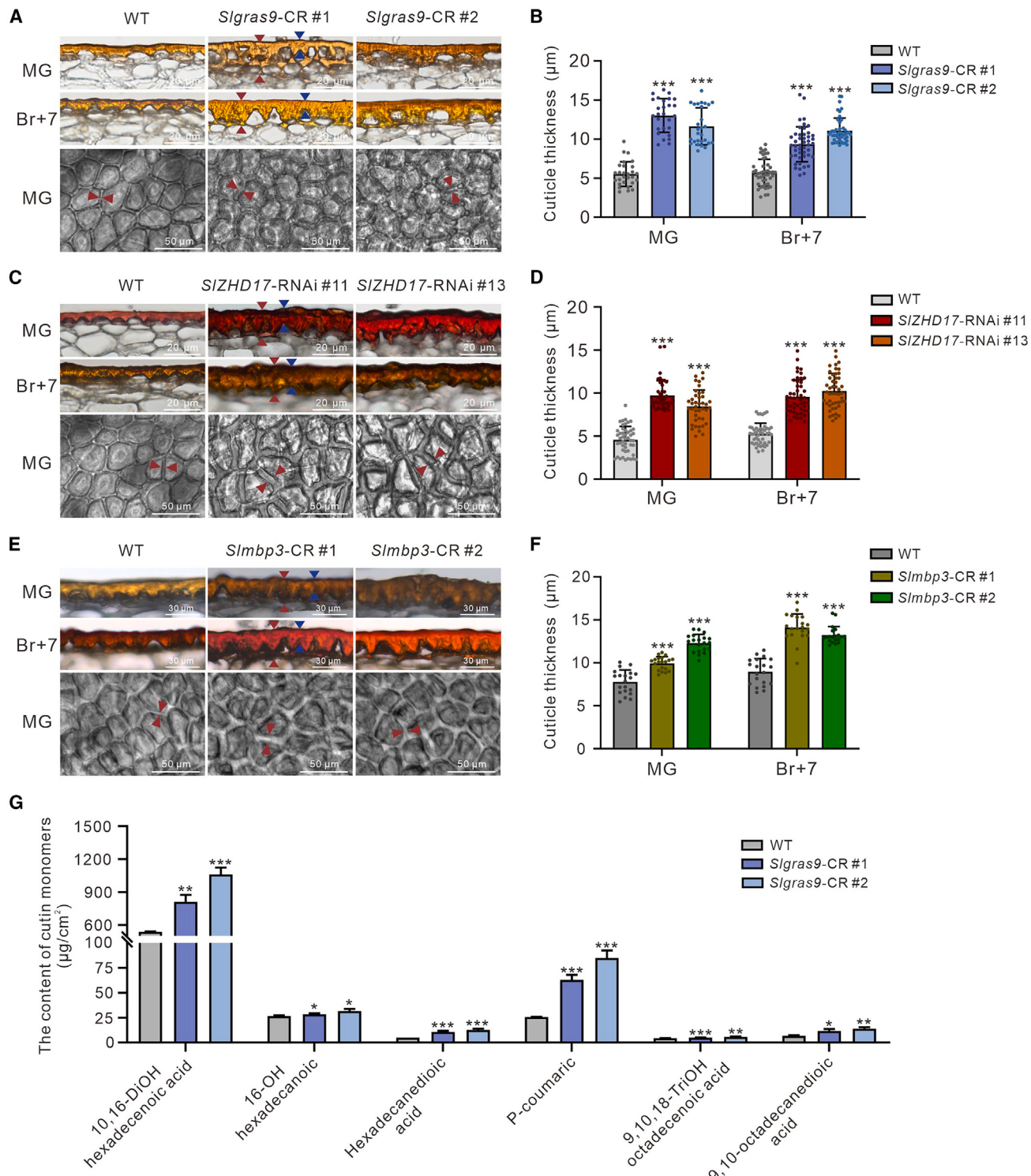


Figure 1. Knockout/knockdown of *SIGRAS9*, *SIZHD17*, or *Slmbp3* results in altered cuticle formation in tomato fruit

(A, C, and E) Microstructure and morphology of the cuticle and epidermal cells upon oil red staining (top) and observation by light microscopy in fruit epidermis of WT, *Slgras9-CR* (A), *SIZHD17-RNAi* (C), and *Slmbp3-CR* (E) lines at mature green (MG) and red ripe (Br+7) stages. Blue and red arrows indicate the cuticle and the permeation of the cuticle into epidermal cells, respectively. The bars represent 20 μm and 30 μm, respectively. The morphology of the epidermal cell of WT, *Slgras9-CR* (A), *SIZHD17-RNAi* (C), and *Slmbp3-CR* (E) was observed by laser scanning confocal microscopy (bottom). The bars represent 50 μm. The red arrow indicates the cutinized cell walls.

(legend continued on next page)

the pavement epidermal cells of *Slgras9*-CR fruit showed more frequent invagination structures (Figure S2C). In addition, SEM observation of the fruit surface showed more irregular surfaces with small dome-like structures and dramatically increased cutinized cell walls between adjacent epidermal cells in *Slgras9*-CR fruit compared to the WT (Figures 1A and S2D). Interestingly, the force needed for piercing the exocarp of *Slgras9*-CR fruit was higher than in the WT, suggesting that the thickened cuticle confers higher resistance to mechanical constraints (Figure S2E). Consistently, the *SIGRAS9*-RNAi lines reproduced all the phenotypes described for *Slgras9*-CR fruit, thereby confirming the active role of *SIGRAS9* in regulating cuticle development (Figures S3A–S3F). Altogether, these findings indicate that the knockout/knockdown of *SIGRAS9* leads to profound changes in cuticle load and structure.

To investigate the effect of *SIGRAS9* loss of function on cuticle biosynthesis, we analyzed cutin components by gas chromatography-mass spectrometry (GC-MS) at the red ripe fruit stage. Compared to that of the WT, the abundance of the main cutin monomers dramatically increased in *Slgras9*-CR and *SIGRAS9*-RNAi fruit (Figures 1G and S3G).

Genome-wide transcriptomic profiling by RNA sequencing (RNA-seq) of mature green (MG) fruit tissue showed that *SIGRAS9* loss of function impacts the expression of a high number of genes, with a total of 4,439 genes being differentially expressed (DEGs) between the WT and *Slgras9*-CR fruit (Data S2). It is worth mentioning that among the DEGs in *Slgras9*-CR fruit, 324 genes encode putative TFs belonging to 26 different families, supporting the idea of a substantial transcriptomic reprogramming in *SIGRAS9*-impaired fruit (Data S3). Of particular interest, two TF genes, *SIZHD17* and *SIMBP3*, previously shown to be direct targets of *SIGRAS9* by DNA affinity purification sequencing (DAP-seq),² were significantly down-regulated in *Slgras9*-CR fruit, prompting us to address their potential role in regulating cutin development in tomato fruit (Figure S4).

Down-regulation of either *SIZHD17* or *SIMBP3* affects cuticle accumulation and deposition in tomato fruit

Interestingly, the down-regulation of *SIZHD17* by RNA (*SIZHD17*-RNAi) and the knockout of *SIMBP3* by CRISPR-Cas9 strategies (*Slmbp3*-CR) both resulted in enhanced cuticle deposition throughout fruit ripening (Figures 1C–1F). SEM and TEM analyses revealed a thickened cuticle in both *SIZHD17*- and *SIMBP3*-impaired lines with notably more invagination structures than in the WT (Figures S5A–S5F). In addition, SEM analysis highlighted the presence of a rough surface entirely covered with small dome-like structures and cutinized cell walls between adjacent epidermal cells in *SIZHD17*- and *SIMBP3*-impaired lines (Figures 1C, 1E, S5E, and S5F). In line with the increased cuticle thickness, the force required to pierce the exocarp was significantly higher for *SIZHD17*-RNAi than for WT fruit (Figure S5G). GC-MS analysis revealed an increased amount of cutin monomers in the cuticle of *SIZHD17*-RNAi and *Slmbp3*-CR fruit, with

a substantial increase in the content of 10,16-dihydroxy-hexadecanoic acid, 16-hydroxy-hexadecanoic acid, and p-coumaric (Figures S5H and S5I). These data support the conclusion that, in addition to *SIGRAS9*, *SIZHD17* and *SIMBP3* are also actively involved in the regulation of cuticle development in tomato fruit.

SIGRAS9, *SIZHD17*, and *SIMBP3* collectively regulate cutin biosynthesis genes

To gain more insight into the molecular mechanisms linking *SIGRAS9* and *SIZHD17* in the regulation of cuticle development, we performed genome-wide transcriptomic profiling of *Slgras9*-CR and *SIZHD17*-RNAi fruit (Data S2 and S4). Mining the RNA-seq profiling data revealed that among the DEGs, the expression of the cutin biosynthesis genes *S/CYP86A69*, *S/CYP77A1*, and *S/GPAT6* displays a similar up-regulation trend at the MG stage in *SIGRAS9*- and *SIZHD17*-impaired lines (Figure 2A). Real-time qPCR analysis confirmed the up-regulation of these cutin biosynthesis genes in both *SIGRAS9*-impaired and *SIZHD17*-deficient fruit at the MG stage (Figures S6A–S6F). Notably, the expression level of *S/CYP86A69*, *S/CYP77A1*, and *S/GPAT6* also increased dramatically in *Slmbp3*-CR fruit, which was confirmed by the transcriptomic profiling of *SIMBP3*-RNAi fruits (Figures S6G–S6I; Table S1). We next investigated whether cutin biosynthesis genes are under the direct regulation of *SIGRAS9*, *SIZHD17*, and *SIMBP3*. Dual-luciferase assays indicated that *SIZHD17* negatively regulates the promoter activity of *S/CYP86A69*, whereas it has no significant effect on *S/CYP77A1* and *S/GPAT6* promoters (Figures 2B and 2C). *SIMBP3* also represses the promoter activity of *S/CYP86A69* (Figure 2D), while *SIGRAS9* shows no effect, suggesting its inability to directly bind to the promoters of this cutin biosynthesis gene (Figure S7). Electrophoretic mobility shift assay (EMSA) experiments confirmed the ability of *SIZHD17* and *SIMBP3* to bind to the *S/CYP86A69* promoter (Figures 2E and 2F). These data indicate that *SIZHD17* and *SIMBP3*, but not *SIGRAS9*, modulate cutin monomer biosynthesis via the direct regulation of *S/CYP86A69*. Furthermore, given the positive regulation of *SIZHD17* by *SIGRAS9*,² we assume that the thickened cutin phenotype observed in *SIGRAS9*-impaired fruit is due to the reduced expression of *SIZHD17* in these lines.

SIGRAS9 and *SIZHD17* have a synergistic effect on cutin formation

We showed above that both *SIGRAS9* and *SIZHD17* play a role in cutin biosynthesis; we then sought to better understand the genetic interaction between these two TFs. Complementation experiments consisting of expressing *SIZHD17* in *SIGRAS9*-deficient lines (3S: *SIZHD17*/*Slgras9*-CR and 3S: *SIZHD17*/*SIGRAS9*-RNAi) resulted in a reduced cuticle thickness compared to non-complemented mutants, although it remained higher than in WT fruit (Figure 3A). It is worth mentioning here that among the complemented *SIGRAS9*-deficient lines generated, we discarded the highly overexpressing ones, retaining only those displaying an *SIZHD17* expression level in the range

(B, D, and F) Cuticle thickness in WT, *Slgras9*-CR (B), *SIZHD17*-RNAi (D), and *Slmbp3*-CR (F) fruit. Data are means (\pm SD) of at least twenty biological replicates. Statistical significance was determined by two-tailed Student's t test. Significant differences are indicated by asterisks (** $p < 0.001$). (G) Quantitative analysis of cutin monomer composition in WT and *Slgras9*-CR fruit at red ripe stage. Data are means (\pm SD) of three biological replicates. Statistical significance was determined by two-tailed Student's t test. Significant differences are indicated by asterisks (* $p < 0.05$, ** $p < 0.01$, and *** $p < 0.001$).

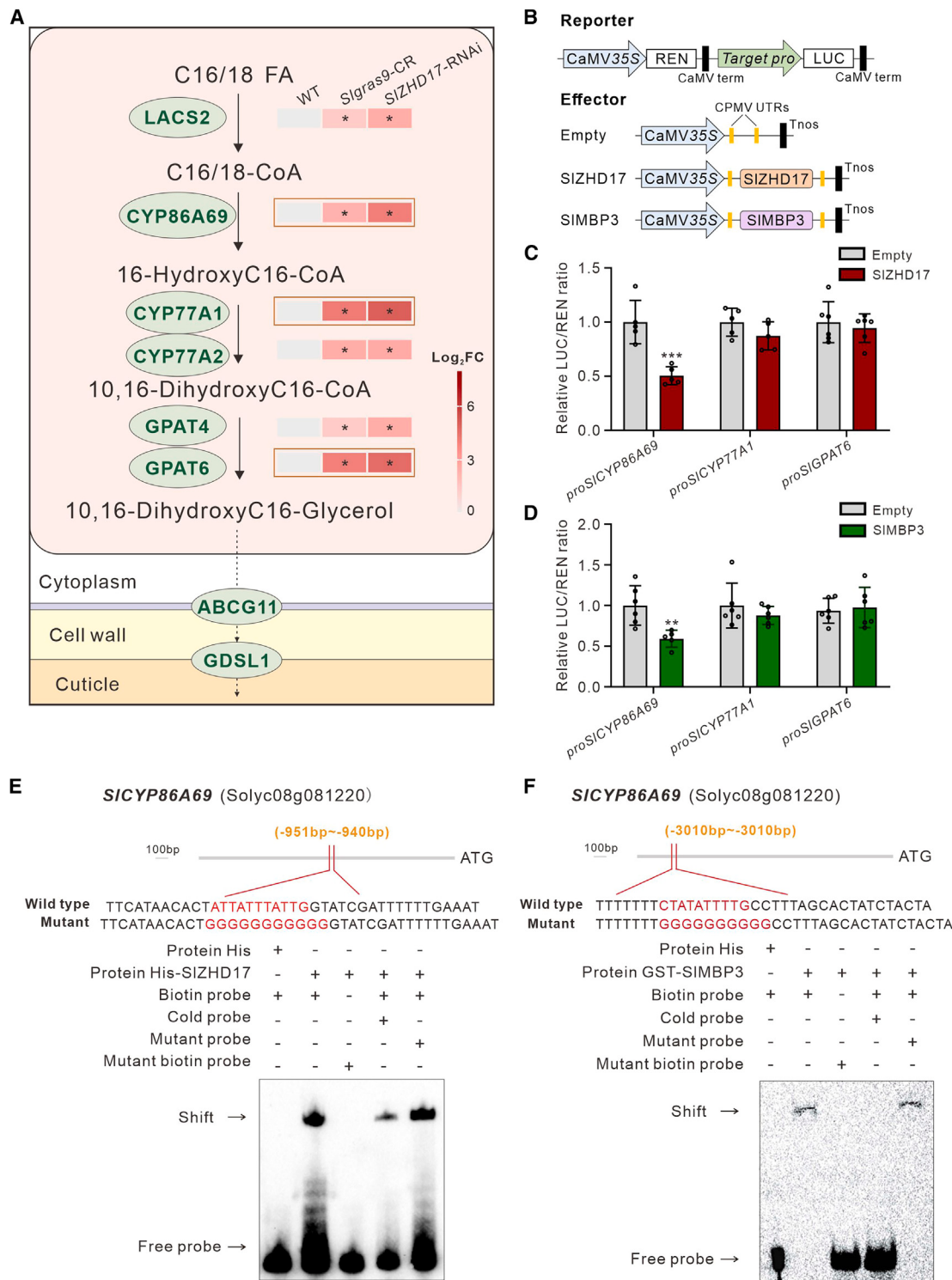


Figure 2. SIGRAS9, SIZHD17, and SIMBP3 collectively regulate genes involved in cutin biosynthesis

(A) Simplified model depicting cutin biosynthesis pathway. The heatmap indicated cutin-associated differentially expressed genes between WT, *Sigras9-CR*, and *SIZHD17-RNAi* fruit extracted from global transcriptome profiling of these lines at the mature green stage.

(B–D) The structural schematic diagrams of the effector and reporter vectors used in dual-luciferase assays. For the reporter construct, promoters of *SICYP86A69*, *SICYP77A1*, and *SIGPAT6* were fused as reporters and the full-length coding sequences of *SIZHD17* and *SIMBP3* as effectors. Regulation of the

(legend continued on next page)

of that observed in the WT (Figure 3B). The data suggest that *SIZHD17* can only partially restore the thickened cuticle phenotype of *SIGRAS9*-deficient fruit. Indeed, cuticle thickness above the pavement epidermal cells and cuticle invaginations were significantly reduced in the fruit of complemented lines (Figures 3C and 3D). Consistently, GC-MS analysis indicated that cutin monomers' content was lower in *SIZHD17*-complemented fruit than in *Slgras9*-CR and *SIGRAS9*-RNAi fruit, albeit still higher than in WT fruit (Figure 3E). Because *SIZHD17* can only partially reverse the thickened cutin phenotype of *SIGRAS9*-deficient fruit, our data suggest that other factors may regulate cutin formation independently of *SIZHD17*.

SIZDH17-SIMBP3 module regulates *S/CYP86A69* expression via synergistic action

Dual-luciferase assays indicated that *SIGRAS9* can activate the expression of *SIMBP3*, while the two proteins showed no ability for interaction (Figures S8A and S8B). On the other hand, RNA-seq and real-time qPCR revealed no changes in the expression of either *SIMBP3* in *SIZHD17*-RNAi or *SIZHD17* in *Slmbp3*-CR, ruling out the possibility of mutual regulation at the transcriptional level of *SIMBP3* by *SIZHD17*, and vice versa (Data S4; Figures S8C and S8D). The ability of *SIMBP3* to interact with *SIZHD17* is clearly demonstrated by both firefly luciferase complementation imaging (LCI) and co-immunoprecipitation (coIP) assays (Figures 4A and 4B). These data sustain the assumption that the interaction between *SIMBP3* and *SIZHD17* may alter the ability of the latter TF to regulate its target genes. Dual-luciferase assay shows that both *SIZHD17* and *SIMBP3* repress *S/CYP86A69* promoter activity (Figure 4C) and that the concomitant presence of both TFs potentiates the inhibitory effect on *S/CYP86A69* expression, indicating that *SIZHD17* and *SIMBP3* function in a synergistic manner.

SIMIXTA-like mitigates the inhibitory action of *SIZHD17* or *SIMBP3* on *S/CYP86A69* promoter

The increased cutin accumulation in *SIGRAS9*-, *SIZHD17*-, and *SIMBP3*-deficient tomato fruit is the opposite of the phenotype reported for the down-regulation of known cutin-related genes, such as *SISHIN3*, *SIMIXTA-like*, *SICD2*, and *SITAGL1*. Strikingly, the transcript accumulation levels of these genes did not show any significant change in *Slgras9*-CR or *SIZHD17*-RNAi fruit, ruling out their regulation at the transcriptional level by *SIGRAS9* and *SIZHD17* (Figures S9A–S9C). We therefore investigated a possible physical interaction at the protein level between *SIGRAS9*, *SIZHD17*, or *SIMBP3* with these cutin-related TFs. LCI and coIP experiments indicated that *SIZHD17* and *SIMBP3* can physically interact with the *SIMIXTA-like* protein (Figures 5A–5D). In addition, *SIZHD17* can interact with *SICD2* and *SITAGL1* (Figures S9D–S9G and S10A). By contrast, *SIGRAS9* failed to show interaction with any of the three TFs (Figures S10B–S10E). We then investigated whether the interaction of *SIMIXTA-like* and *SICD2* with *SIZHD17*

or *SIMBP3* affects their ability to regulate the expression of the target genes. EMSA experiments indicated that the binding of *SIZHD17* to the promoter fragment of *S/CYP86A69* gradually decreases and eventually disappears in the presence of increased concentrations of *SIMIXTA-like* or *SICD2* proteins, suggesting that the binding activity of *SIZHD17* is hindered by *SIMIXTA-like* or *SICD2* proteins in a dose-dependent manner (Figures 5E and S11A). Similarly, the binding of *SIMBP3* to the promoter fragment of *S/CYP86A69* gradually decreases with the increase in *SIMIXTA-like* protein concentration (Figure 5F). By contrast, *SITAGL1* had no significant effect on the binding ability of *SIZHD17* to the *S/CYP86A69* promoter (Figure S11B). We also tested the binding ability of *SIMIXTA-like*, *SICD2*, and *SITAGL1* to the *S/CYP86A69* promoter, showing that none of these TFs can directly bind to the promoter fragments of this gene (Figures S11C–S11E). The ability of *SIMIXTA-like* to repress the binding of *SIZHD17* and *SIMBP3* to the *S/CYP86A69* promoter prompted us to examine its ability to regulate the activity of this target promoter. Dual-luciferase assays in tobacco leaves showed that the inhibitory activity of *SIZHD17* or *SIMBP3* on the *S/CYP86A69* promoter is weakened in the presence of *SIMIXTA-like* (Figure 5G). On the other hand, the inhibitory effect of *SIZHD17* on the *S/CYP86A69* promoter is mitigated by *SICD2* (Figure S11F). Altogether, the protein-protein interaction experiments indicated that *SIMIXTA-like* and *SICD2* can weaken the inhibitory effect and binding activity of *SIZHD17* and *SIMBP3* on the *S/CYP86A69* gene promoter, indicating that these two TFs regulate cutin biosynthesis antagonistically to *SIZHD17* and *SIMBP3*.

Impaired expression of *SIGRAS9*, *SIZHD17*, or *SIMBP3* results in enhanced resistance to fruit fungal rot during postharvest storage

Fruit cuticle plays an important role in improving shelf life and protecting against pathogens in pre- and postharvest tomato fruit. Postharvest storage experiments revealed that the knockout or knockdown of *SIGRAS9*, *SIZHD17*, or *SIMBP3* results in an extended shelf life (Figure S12A). We also evaluated fruit susceptibility to *Botrytis cinerea* infection, which is known to lead to serious losses of tomato crops. The symptoms of advanced infection with growing mycelium were observed in WT fruit at 7 days post-inoculation, whereas these symptoms were milder in *Slgras9*-CR, *SIGRAS9*-RNAi, *SIZHD17*-RNAi, and *Slmbp3*-CR fruit (Figure S12B). Consistently, assessing *Botrytis cinerea* biomass as a pathogen growth marker by real-time qPCR indicated significantly reduced fungal propagation in *Slgras9*-CR, *SIGRAS9*-RNAi, *SIZHD17*-RNAi, and *Slmbp3*-CR fruit compared to the WT (Figure S12C).

DISCUSSION

The importance of the cuticle has been largely overlooked in breeding strategies despite its key role in reducing water loss,

abovementioned gene promoters by *SIZHD17* (C) and *SIMBP3* (D) based on dual-luciferase assay. The empty effector was regarded as a calibrator (set as 1). Data are means (\pm SD) of at least five biological replicates. Statistical significance was determined by two-tailed Student's t test. The significant differences are indicated by asterisks (** $p < 0.01$ and *** $p < 0.001$).

(E and F) EMSA experiments for assessing *SIZHD17* (E) and *SIMBP3* (F) binding to *S/CYP86A69* promoter region. The biotin-labeled DNA probe incubated with TF-His protein was used as a negative control. –, absence; +, presence.

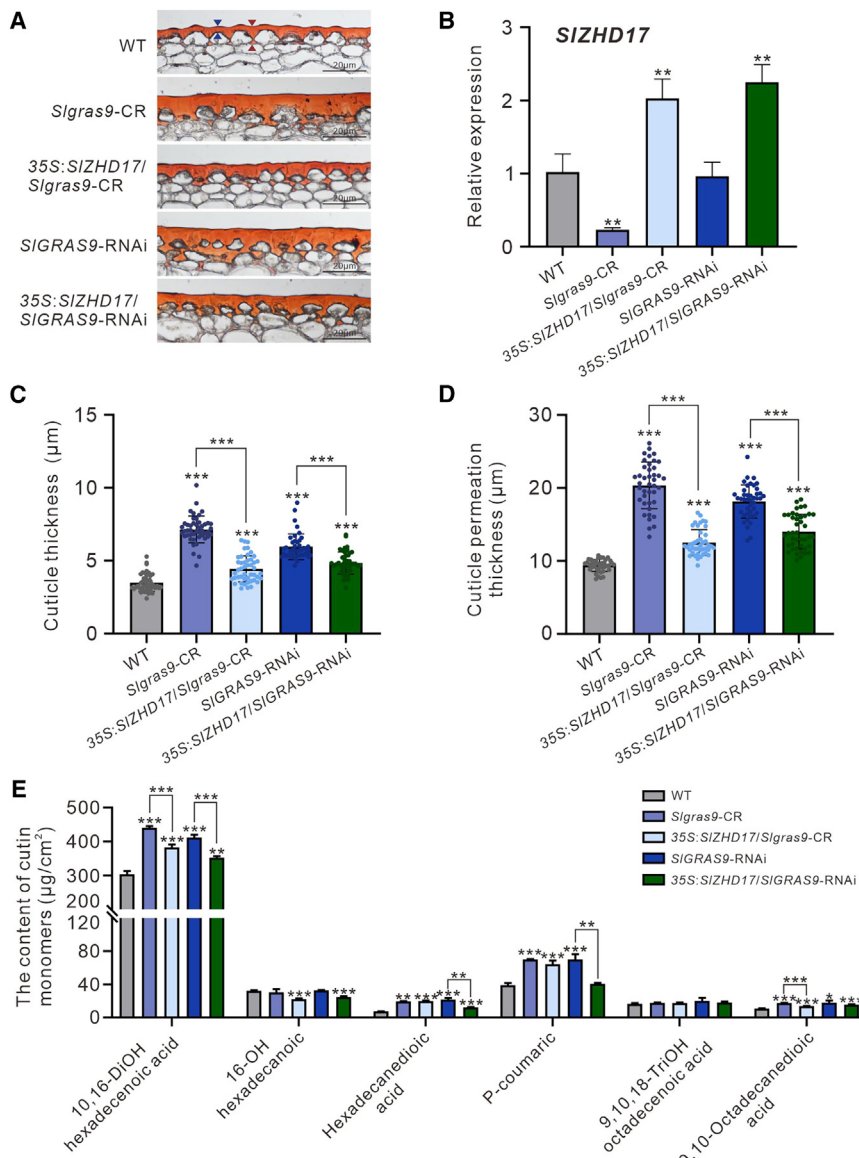


Figure 3. Complementation experiments of the fruit cuticle phenotype in tomato Sigras9-CR or SIGRAS9-RNAi lines

(A) Oil red staining was used to analyze differences in cuticle deposition in WT, Sigras9-CR, 35S: SIZHD17/Sigras9-CR, SIGRAS9-RNAi, and 35S: SIZHD17/SIGRAS9-RNAi fruit at mature green stage. The bars represent 20 μm .

(B) The relative expression of SIZHD17 in WT, Sigras9-CR, 35S: SIZHD17/Sigras9-CR, SIGRAS9-RNAi, and 35S: SIZHD17/SIGRAS9-RNAi leaves. The transcript level in WT was set as 1. Data are means ($\pm\text{SD}$) of three biological replicates. Statistical significance was determined by two-tailed Student's t test. Significant differences are indicated by asterisks (** $p < 0.01$).

(C and D) Cuticle thickness (C) and cuticle permeation (D) in WT, Sigras9-CR, 35S: SIZHD17/Sigras9-CR, SIGRAS9-RNAi, and 35S: SIZHD17/SIGRAS9-RNAi fruit. Data are means ($\pm\text{SD}$) of at least twenty biological replicates. Statistical significance was determined by two-tailed Student's t test. Significant differences are indicated by asterisks (** $p < 0.001$).

(E) Quantification of cutin monomers' compositions in WT, Sigras9-CR, 35S: SIZHD17/Sigras9-CR, SIGRAS9-RNAi, and 35S: SIZHD17/SIGRAS9-RNAi fruit. Data are means ($\pm\text{SD}$) of three biological replicates. Statistical significance was determined by two-tailed Student's t test. Significant differences are indicated by asterisks (* $p < 0.05$, ** $p < 0.01$, and *** $p < 0.001$).

preventing peel cracking, and controlling postharvest decay.^{52,53} In tomato fruit, a thick cuticle provides a protective barrier against biotic and abiotic aggressors and confers important quality traits like peel brightness and better postharvest behavior. Most insights into cuticle development have been obtained from studies of loss-of-function mutants that exhibit cuticle defects in either model or crop species.^{33,39} Several regulatory components affecting the formation of the tomato cuticle have been identified, including SISHIN3, SIMIXTA-like, SICD2, SITAGL1, SINOR-like1, SIWoolly, SIMYB31, and SIMYB72.^{31,38,45–50} The cuticle is synthesized by the epidermal cell layer and the transcriptional activity of the SIMIXTA-like, SICD2, or SITAGL1 gene is thought to be essential for epidermal-related differentiation/developmental processes.^{33,38,46,48,54} The close relationship between epidermal cell differentiation and cuticle formation has been

demonstrated in *Arabidopsis*.⁵⁵ Our work uncovers the existence of a multipartite module regulating cutin formation and unveils the complex interactions between its components that enable the fine-tuning of this metabolic pathway (Figure 6). While quite a few studies have explored the mutual roles of the myriads of TFs that collectively regulate cutin formation, our data shed unprecedented light on the complexity

of the interactions between multiple TFs involved in fine-tuning the cutin metabolic pathway. Besides the already known regulators SISHIN3, SIMIXTA-like, SICD2, SITAGL1, and SINOR-like1, we demonstrate that three additional TFs, namely SIGRAS9, SIZHD17, and SIMBP3, take part in the regulatory network of this metabolic pathway. Deciphering the complex interactions between these regulators reveals the functional links between the newly discovered TFs and those previously described. In particular, we show that these regulators function in both synergistic and antagonistic modes to control cutin formation in tomato fruit.

As depicted in the tentative model proposed (Figure 6), the complex regulatory network controlling cutin biosynthesis operates through interacting TFs working both synergistically and antagonistically. S/CYP86A69 mediates a key step of cutin biosynthesis and is the central target of this regulatory module.

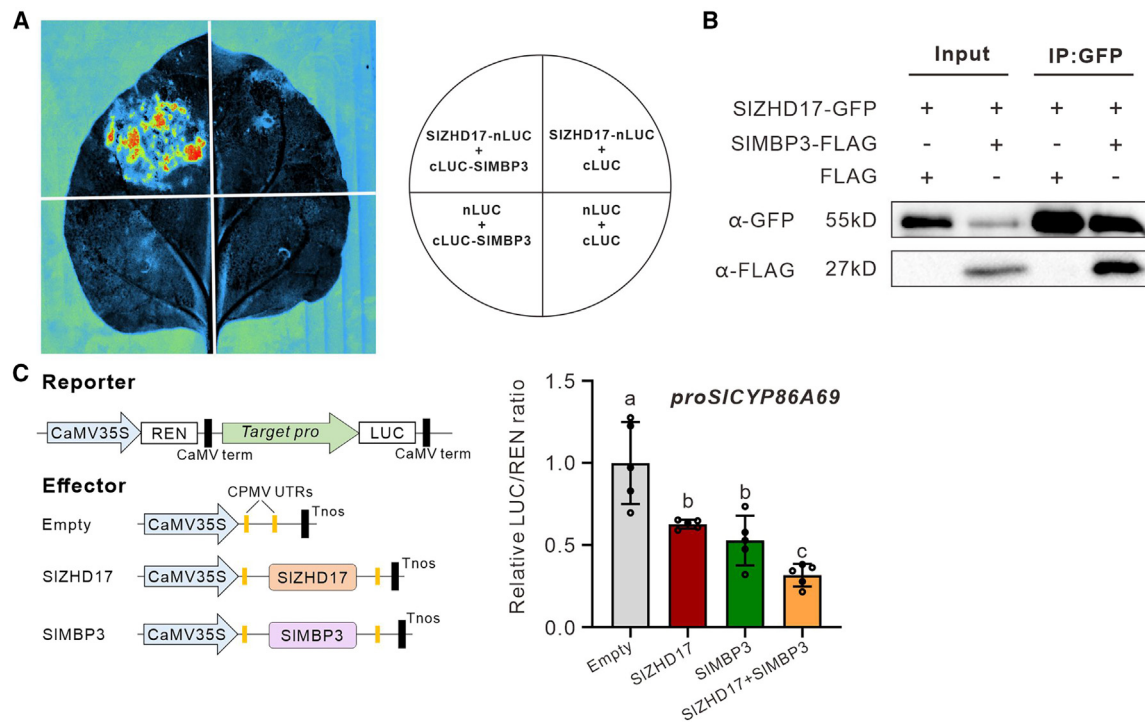


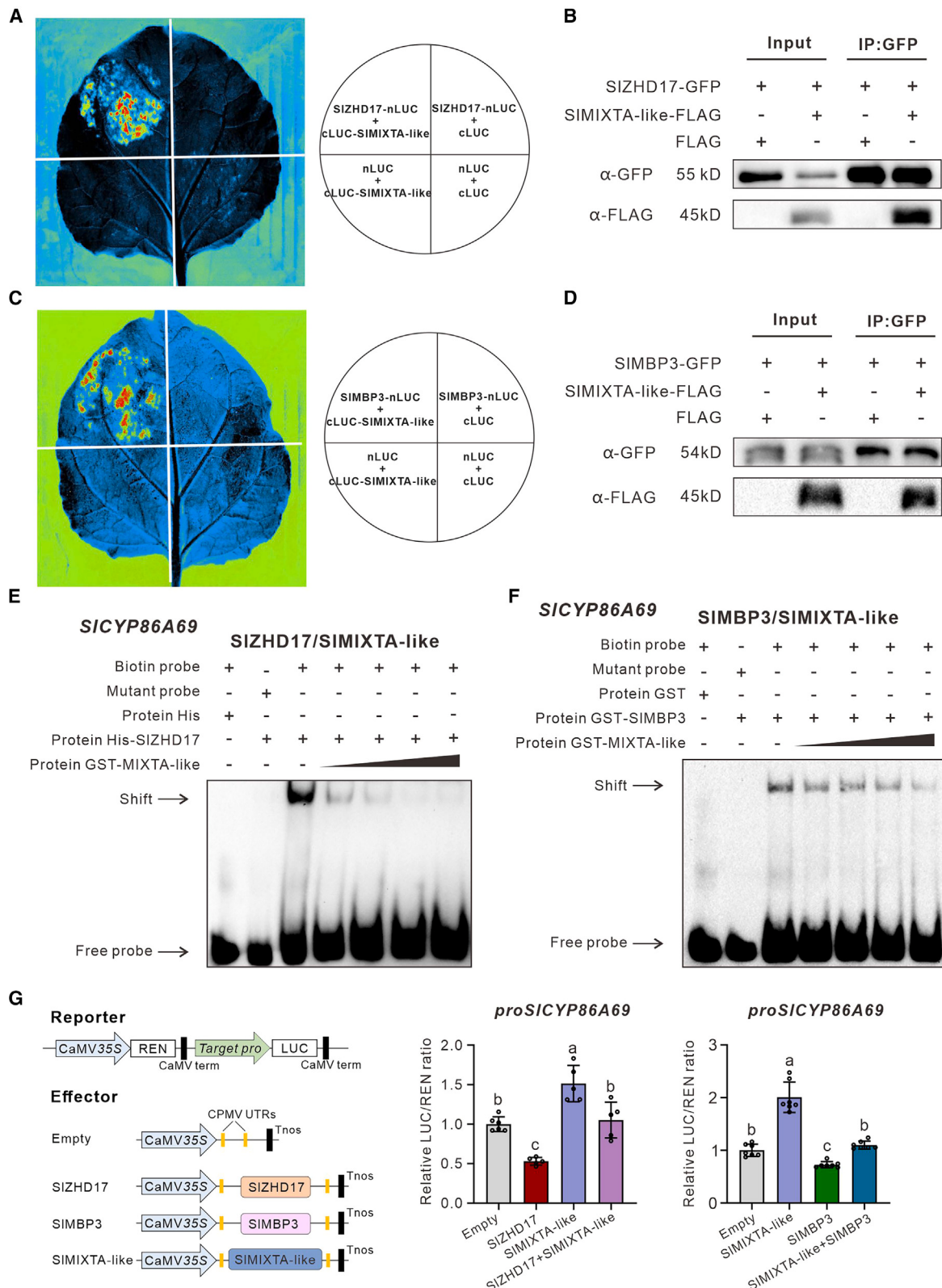
Figure 4. SIMBP3 and SIZHD17 synergistically regulate the expression of S/CYP86A69

(A) Protein-protein interaction of SIZHD17 with SIMBP3 was analyzed by firefly luciferase complementation imaging assay in tobacco leaves.
(B) Co-immunoprecipitation assay of the protein-protein interaction of SIZHD17 with SIMBP3. Precipitates were detected with anti-GFP and anti-FLAG antibodies.
(C) Structural schematic diagrams of the effector and reporter vectors used in dual-luciferase assays. For the reporter construct, the promoter of *S/CYP86A69* was fused to the reporter, and the full-length coding sequence of *SIZHD17* and *SIMBP3* was constructed into the effector vectors. The reporter was co-expressed with either the SIZHD17 effector alone or the SIMBP3 effector alone or with SIZHD17 in combination with SIMBP3. The Luciferase/Renilla (LUC/REN) ratio of the empty effector group was regarded as the calibrator (set as 1). Each column represents the mean values of at least five biological replicates, and error bars represent the standard error values. The significant differences are indicated with letters ($p < 0.05$, Duncan's multiple range test).

S/CYP86A69 encodes a cytochrome P450 from the CYP86A subgroup, which has fatty acid hydroxylase activity involved in the formation of cutin monomers.³⁸ Mutants defective in *s/cyp86a69* exhibit a thin cuticle, as well as a short shelf life and reduced resistance to black rot disease.^{37,38} We show that tomato lines impaired in the expression of *SIGRAS9* and *SIZHD17* exhibit thicker cuticles and that SIZHD17, but not SIGRAS9, can directly inhibit *S/CYP86A69* expression. Upstream of the regulatory network, SIGRAS9 activates the expression of *SIZHD17*, which negatively regulates the *S/CYP86A69* gene through direct binding to its promoter. SIZHD17 interacts with SIMBP3 at the protein level to synergistically repress the expression of *S/CYP86A69*. Conversely, the interaction of SIZHD17 with either of the two positive regulators of cutin formation, SIMIXTA-like or SICD2, prevents its binding to the *S/CYP86A69* promoter, thereby promoting cutin biosynthesis. Notably, SIMIXTA-like promotes *S/CYP86A69* transcription, although it lacks the ability to directly bind its promoter, which is consistent with an indirect regulation of *S/CYP86A69* by SIMIXTA-like. Furthermore, it cannot be ruled out that SIMIXTA-like interacts with other regulatory factors to jointly regulate the expression of the *S/CYP86A69* gene. By contrast, SIMBP3 can repress *S/CYP86A69* transcription through direct

binding to its promoter, and the repressive action of SIMBP3 on this biosynthetic gene is potentiated by its interaction with SIZHD17. On the other hand, the repressive activity of SIMBP3 on the *S/CYP86A69* promoter is hampered by its interaction with SIMIXTA-like.

Interestingly, the thickened cuticle observed in *SIGRAS9* and *SIZHD17* down-regulated fruit is opposite to the phenotype exhibited by tomato lines down-regulated in the *SISHIN3*, *SIMIXTA-like*, *SICD2*, or *SITAGL1* gene.^{38,45–48} *SISHIN3* and *SIMIXTA-like* are important regulators of cuticle formation, and the knockdown of any of the two genes leads to a significant decrease in cutin accumulation associated with reduced storage tolerance and postharvest pathogen resistance.^{38,46} *SICD2* and *SITAGL1* have been also reported to positively contribute to cutin accumulation in tomato fruit^{45,48}; however, no significant change in the expression of these genes was observed in *SIGRAS9* and *SIZHD17* down-regulated fruit. We show that SIMIXTA-like, SICD2, and SITAGL1 are able to physically interact with SIZHD17 but not SIGRAS9. Dual-luciferase and EMSA experiments revealed that the inhibitory effects of SIZHD17 on the *S/CYP86A69* promoter are hindered by its interaction with SIMIXTA-like. Overall, the outcome of the study supports a model in which SIZHD17 and SIMBP3 act synergistically to



(legend on next page)

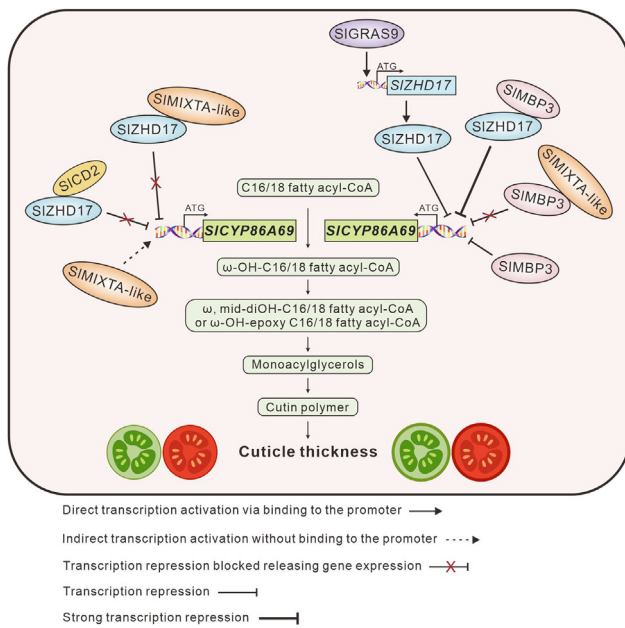


Figure 6. Proposed model shows that the SIGRAS9-SIZHD17-SIMBP3-SIMIXTA-like regulatory mode controls the cutin accumulation in tomato fruit

These data support that multiple interacting transcription factors worked both synergistically and antagonistically to form a complex regulatory network to control cutin biosynthesis. SIGRAS9 located upstream in the regulatory network directly targets SIZHD17, which can repress the transcription of the *S/CYP86A69* gene, encoding an essential enzyme of cutin biosynthesis, through direct binding to its promoter. Similarly, SIMBP3 can negatively regulate the *S/CYP86A69* gene through direct binding to its promoter, and SIZHD17 and SIMBP3 can synergistically repress the expression of *S/CYP86A69* through protein-protein interaction. By contrast, the protein-protein interaction between SIZHD17 and SIMIXTA-like or SICD2, two positive regulators of cutin formation, prevents its binding to *S/CYP86A69* promoter. On the other hand, the repressive activity of SIMBP3 on the promoter of the *S/CYP86A69* gene is hampered by its interaction with SIMIXTA-like, thereby promoting cutin biosynthesis.

repress cutin biosynthesis, while SIMIXTA-like and SICD2 act antagonistically to SIZHD17 and SIMBP3 on this metabolic pathway (Figure 6).

By expanding our knowledge of the mechanisms and factors underpinning the regulation of cutin formation, our study defines additional targets for precision breeding strategies aiming to improve cuticle-related traits without compromising the flavor

qualities of fleshy fruit. Similarly, significant alterations in cuticle deposition and epidermal cell morphology were also observed in *SIGRAS9*, *SIZHD17*, and *SIMBP3* down-regulated lines, implying that *SIGRAS9*, *SIZHD17*, and *SIMBP3* might be important regulators linking epidermal cell patterning and cuticle development. Furthermore, it cannot be excluded that the complexes formed by the interactions between SICD2, SITAGL1, SIZHD17, and SIMBP3 might be involved in other aspects of fruit development that are not limited to cutin formation. This hypothesis could be validated by creating multiple mutants of these key regulatory factors. Notably, impairing *SIGRAS9*, *SIZHD17*, or *SIMBP3* expression led to a significant increase in sugar content in tomato fruit,² implying that these genes may offer potential targets for improving the shelf life and flavor quality of tomato fruit. Taken together, the results of our study unravel the diversified modes for the regulation of cutin formation mediated by the *SIGRAS9*-*SIZHD17*-*SIMBP3*-*SIMIXTA-like* regulatory module. This modular regulation mechanism allows tight control of target genes involved in cutin formation pathways. While providing a renewed and largely enriched view of the mechanisms underpinning the control of cuticle development, our findings also define important genetic loci for molecular breeding of cuticle-associated traits in tomato and potentially other horticultural crops.

Limitations of the study

Tomato lines with multiple mutations proved very difficult to obtain, as the mutation of each of the three genes affects seed germination efficiency, and their cumulative effect in a single line has precluded the generation of triple mutants. Furthermore, in order to broaden the breeding potential of these regulatory genes, it would be important to address the functional conservation of these TFs in other horticultural species beyond tomato.

RESOURCE AVAILABILITY

Lead contact

Requests for further information and resources should be directed to and will be fulfilled by the lead contact, Baowen Huang (huangbaowen2022@cqu.edu.cn).

Materials availability

All plant materials and plasmids generated in this paper will be shared by the lead contact upon request. This study did not generate new unique reagents.

Data and code availability

- The raw RNA-seq data have been deposited in the Genome Sequence Archive of the National Genomics Data Center, Beijing Institute of

Figure 5. SIMIXTA-like impairs the repressing activity of SIZHD17 or SIMBP3 on the *S/CYP86A69* promoter by abolishing its binding ability (A and C) Protein-protein interaction of SIZHD17 (A) or SIMBP3 (C) with SIMIXTA-like was analyzed by firefly luciferase complementation imaging assay in tobacco leaves. (B and D) Co-immunoprecipitation assay of the protein-protein interaction of SIZHD17 (B) or SIMBP3 (D) with SIMIXTA-like. Precipitates were detected with anti-GFP and anti-FLAG antibodies. (E and F) The effect of the presence of SIMIXTA-like on the binding ability of SIZHD17 (E) and SIMBP3 (F) to *S/CYP86A69* promoter fragment. Biotin probes were incubated with His-SIZHD17 or GST-SIMBP3 alone or together with GST-SIMIXTA-like. The right black triangle indicates an increased amount of SIMIXTA-like protein. The biotin-labeled DNA probe incubated with TF-His protein was used as a negative control. –, absence; +, presence. (G) Structural schematic diagrams of the effector and reporter vectors used in dual-luciferase assays. For the reporter construct, the *S/CYP86A69* promoter was fused to the reporter, and the full-length coding sequences of *SIMIXTA-like*, *SIZHD17*, or *SIMBP3* were constructed into the effector vectors. The reporter was co-expressed with either the *SIMIXTA-like* effector alone or the *SIZHD17/SIMBP3* effector alone or with *SIMIXTA-like* in combination with *SIZHD17/SIMBP3*. The LUC/REN ratio of the empty effector group was regarded as the calibrator (set as 1). Each column represents the mean values of at least five biological replicates, and error bars represent standard error values. Significant differences are indicated with letters ($p < 0.05$, Duncan's multiple range test).

Genomics, Chinese Academy of Sciences (GSA: PRJCA018221), which can be accessed publicly at <https://ngdc.cncb.ac.cn/gsa>.

- This paper does not report original code.
- Any additional information required to reanalyze the data reported in this paper is available from the lead contact upon request.

ACKNOWLEDGMENTS

This work was sponsored by the National Natural Science Foundation of China (nos. 32230092, 32202563, and 32372403), the New Youth Innovation Talent Project of Chongqing (2024NSCQ-qncxX0339), the Fundamental Research Funds for the Central Universities (no. 2024IAIS-ZX005), the National Key Research and Development Program of China (no. 2022YFD2100105), the Natural Science Foundation of Chongqing (CSTB2023NSCQ-MSX0529), the Entrepreneurship and Innovation Support Program of Overseas Students of Chongqing (cx2023106), the Chongqing Technology Innovation and Application Development Project (cstc2012jscxgksbX0021 and cstc2019jscxdxwtBX0027), and the Chongqing Modern Agricultural Industry Technology System (CQMAITS202302).

AUTHOR CONTRIBUTIONS

B.H., Z.L., M.B., Y. Liu, and Y.S. designed the experiments; Y.S., C.D., X.L., Y.W., Y.P., D.S., W.L., Y. Lin, R.L., and J.H. performed the experiments; B.H., Z.L., Y. Liu, Y.C., G.A., and Y.H. provided experimental assistance; Y.S. wrote the manuscript; and B.H., J.P., Z.L., M.B., and Y. Liu revised the paper. All authors read and approved the final manuscript.

DECLARATION OF INTERESTS

The authors declare no competing interests.

STAR★METHODS

Detailed methods are provided in the online version of this paper and include the following:

- KEY RESOURCES TABLE
- EXPERIMENTAL MODEL AND STUDY PARTICIPANT DETAILS
- METHOD DETAILS
 - Generation of plant materials
 - RNA extraction, cDNA synthesis, real-time qPCR and RNA-seq
 - Fruit pericarp microstructure observation
 - Cutin monomer analyses
 - Shelf-life analysis
 - *Botrytis cinerea* infection
 - Dual-luciferase assays
 - Electrophoretic mobility shift assay
 - Firefly luciferase complementation imaging (LCI) assay
 - Co-immunoprecipitation assays (coIP)
- QUANTIFICATION AND STATISTICAL ANALYSIS

SUPPLEMENTAL INFORMATION

Supplemental information can be found online at <https://doi.org/10.1016/j.celrep.2025.115258>.

Received: September 24, 2024

Revised: October 29, 2024

Accepted: January 13, 2025

Published: January 31, 2025

REFERENCES

1. Huang, W., Peng, S., Xian, Z., Lin, D., Hu, G., Yang, L., Ren, M., and Li, Z. (2017). Overexpression of a tomato miR171 target gene *SIGRAS24* imparts multiple agronomical traits via regulating gibberellin and auxin homeostasis. *Plant Biotechnol. J.* **15**, 472–488.
2. Shi, Y., Hu, G., Wang, Y., Liang, Q., Su, D., Lu, W., Deng, W., Bouzayen, M., Liu, Y., Li, Z., and Huang, B. (2024). The SIGRAS9-SIZHD17 transcriptional cascade regulates chlorophyll and carbohydrate metabolism contributing to fruit quality traits in tomato. *New Phytol.* **241**, 2540–2557.
3. Tieman, D., Zhu, G., Resende, M.F.R., Jr., Lin, T., Nguyen, C., Bies, D., Rambla, J.L., Beltran, K.S.O., Taylor, M., Zhang, B., et al. (2017). A chemical genetic roadmap to improved tomato flavor. *Science* **355**, 391–394.
4. Huang, B., Hu, G., Wang, K., Frasse, P., Maza, E., Djari, A., Deng, W., Pirrello, J., Burlat, V., Pons, C., et al. (2021). Interaction of two MADS-box genes leads to growth phenotype divergence of all-flesh type of tomatoes. *Nat. Commun.* **12**, 6892.
5. Dominguez, E., Fernández, M.D., Hernández, J.C.L., Parra, J.P., España, L., Heredia, A., and Cuartero, J. (2012). Tomato fruit continues growing while ripening, affecting cuticle properties and cracking. *Physiol. Plantarum* **146**, 473–486.
6. Yang, L., Huang, W., Xiong, F., Xian, Z., Su, D., Ren, M., and Li, Z. (2017). Silencing of *SIP1*, which encodes a pectate lyase in tomato, confers enhanced fruit firmness, prolonged shelf-life and reduced susceptibility to grey mould. *Plant Biotechnol. J.* **15**, 1544–1555.
7. Shinozaki, Y., Nicolas, P., Fernandez-Pozo, N., Ma, Q., Evanich, D.J., Shi, Y., Xu, Y., Zheng, Y., Snyder, S.I., Martin, L.B.B., et al. (2018). High-resolution spatiotemporal transcriptome mapping of tomato fruit development and ripening. *Nat. Commun.* **9**, 364.
8. Eriksson, E.M., Bovy, A., Manning, K., Harrison, L., Andrews, J., De Silva, J., Tucker, G.A., and Seymour, G.B. (2004). Effect of the colorless non-ripening mutation on cell wall biochemistry and gene expression during tomato fruit development and ripening. *Plant Physiol.* **136**, 4184–4197.
9. Fujisawa, M., Nakano, T., and Ito, Y. (2011). Identification of potential target genes for the tomato fruit-ripening regulator RIN by chromatin immunoprecipitation. *BMC Plant Biol.* **11**, 26.
10. Fujisawa, M., Nakano, T., Shima, Y., and Ito, Y. (2013). A large-scale identification of direct targets of the tomato MADS box transcription factor RIPENING INHIBITOR reveals the regulation of fruit ripening. *Plant Cell* **25**, 371–386.
11. Quinet, M., Angosto, T., Yuste-Lisbona, F.J., Blanchard-Gros, R., Bigot, S., Martinez, J.P., and Lutts, S. (2017). NAC-NOR mutations in tomato Penjar accessions attenuate multiple metabolic processes and prolong the fruit shelf life. *Food Chem.* **259**, 234–244.
12. Quinet, M., Angosto, T., Yuste-Lisbona, F.J., Blanchard-Gros, R., Bigot, S., Martinez, J.P., and Lutts, S. (2019). Tomato fruit development and metabolism. *Front. Plant Sci.* **10**, 1554.
13. Seymour, G.B., Manning, K., Eriksson, E.M., Popovich, A.H., and King, G.J. (2002). Genetic identification and genomic organization of factors affecting fruit texture. *J. Exp. Bot.* **53**, 2065–2071.
14. Shi, Y., Vrebalov, J., Zheng, H., Xu, Y., Yin, X., Liu, W., Liu, Z., Sorensen, I., Su, G., Ma, Q., et al. (2021). A tomato LATERAL ORGAN BOUNDARIES transcription factor, SILOB1, predominantly regulates cell wall and softening components of ripening. *Proc. Natl. Acad. Sci. USA* **118**, e2102486118.
15. Petit, J., Bres, C., Reynoud, N., Lahaye, M., Marion, D., Bakan, B., and Rothan, C. (2021). Unraveling cuticle formation, structure, and properties by using tomato genetic diversity. *Front. Plant Sci.* **12**, 778131.
16. Li, R., Sun, S., Wang, H., Wang, K., Yu, H., Zhou, Z., Xin, P., Chu, J., Zhao, T., Wang, H., et al. (2020). FIS1 encodes a GA2-oxidase that regulates fruit firmness in tomato. *Nat. Commun.* **11**, 5844.
17. Zhang, L., Zhu, M., Ren, L., Li, A., Chen, G., and Hu, Z. (2018). The SIFSR gene controls fruit shelf-life in tomato. *J. Exp. Bot.* **69**, 2897–2909.
18. Petit, J., Bres, C., Just, D., Garcia, V., Mauxion, J.P., Marion, D., Bakan, B., Joubès, J., Domergue, F., and Rothan, C. (2014). Analyses of tomato fruit brightness mutants uncover both cutin-deficient and cutin-abundant

- mutants and a new hypomorphic allele of GDSL Lipase. *Plant Physiol.* 164, 888–906.
19. Romero, P., and Rose, J.K.C. (2019). A relationship between tomato fruit softening, cuticle properties and water availability. *Food Chem.* 295, 300–310.
 20. España, L., Heredia-Guerrero, J.A., Segado, P., Benítez, J.J., Heredia, A., and Domínguez, E. (2014). Biomechanical properties of the tomato (*Solanum lycopersicum*) fruit cuticle during development are modulated by changes in the relative amounts of its components. *New Phytol.* 202, 790–802.
 21. Brüggenwirth, M., and Knoche, M. (2017). Cell wall swelling, fracture mode, and the mechanical properties of cherry fruit skins are closely related. *Planta* 245, 765–777.
 22. Fich, E.A., Segerson, N.A., and Rose, J.K.C. (2016). The plant polyester cutin: biosynthesis, structure, and biological roles. *Annu. Rev. Plant Biol.* 67, 207–233.
 23. Li-Beisson, Y., Pollard, M., Sauveplane, V., Pinot, F., Ohlrogge, J., and Beisson, F. (2009). Nanoridges that characterize the surface morphology of flowers require the synthesis of cutin polyester. *Proc. Natl. Acad. Sci. USA* 106, 22008–22013.
 24. Saladié, M., Matas, A.J., Isaacson, T., Jenks, M.A., Goodwin, S.M., Niklas, K.J., Xiaolin, R., Labavitch, J.M., Shackel, K.A., Fernie, A.R., et al. (2007). A reevaluation of the key factors that influence tomato fruit softening and integrity. *Plant Physiol.* 144, 1012–1028.
 25. Kosma, D.K., Parsons, E.P., Isaacson, T., Lü, S., Rose, J.K.C., and Jenks, M.A. (2010). Fruit cuticle lipid composition during development in tomato ripening mutants. *Physiol. Plantarum* 139, 107–117.
 26. Jenkin, S., and Molina, I. (2015). Isolation and compositional analysis of plant cuticle lipid polyester monomers. *J. Vis. Exp.* 105, 53386.
 27. Fernández-Muñoz, R., Heredia, A., and Domínguez, E. (2022). The role of cuticle in fruit shelf-life. *Curr. Opin. Biotechnol.* 78, 102802.
 28. Segado, P., Domínguez, E., and Heredia, A. (2015). Ultrastructure of the epidermal cell wall and cuticle of tomato fruit (*Solanum lycopersicum* L.) during development. *Plant Physiol.* 170, 935–946.
 29. Matas, A.J., López-Casado, G., Cuartero, J., and Heredia, A. (2005). Relative humidity and temperature modify the mechanical properties of isolated tomato fruit cuticles. *Am. J. Bot.* 92, 462–468.
 30. López-Casado, G., Matas, A.J., Domínguez, E., Cuartero, J., and Heredia, A. (2007). Biomechanics of isolated tomato (*Solanum lycopersicum* L.) fruit cuticles: the role of the cutin matrix and polysaccharides. *J. Exp. Bot.* 58, 3875–3883.
 31. Liu, G.S., Huang, H., Grierson, D., Gao, Y., Ji, X., Peng, Z.Z., Li, H.L., Niu, X.L., Jia, W., He, J.L., et al. (2024). NAC transcription factor SINOR-like1 plays a dual regulatory role in tomato fruit cuticle formation. *J. Exp. Bot.* 75, 1903–1918.
 32. Yeats, T.H., Buda, G.J., Wang, Z., Chehanovsky, N., Moyle, L.C., Jetter, R., Schaffer, A.A., and Rose, J.K.C. (2012). The fruit cuticles of wild tomato species exhibit architectural and chemical diversity, providing a new model for studying the evolution of cuticle function. *Plant J.* 69, 655–666.
 33. Petit, J., Bres, C., Mauxion, J.P., Bakan, B., and Rothan, C. (2017). Breeding for cuticle-associated traits in crop species: traits, targets, and strategies. *J. Exp. Bot.* 68, 5369–5387.
 34. Elejalde-Palmett, C., Martínez San Segundo, I., Garroum, I., Charrier, L., De Bellis, D., Muccioli, A., Guerault, A., Liu, J., Zeisler-Diehl, V., Aharoni, A., et al. (2021). ABCG transporters export cutin precursors for the formation of the plant cuticle. *Curr. Biol.* 31, 2111–2123.
 35. Kurdyukov, S., Faust, A., Nawrath, C., Bár, S., Voisin, D., Efremova, N., Franke, R., Schreiber, L., Saedler, H., Métraux, J.P., and Yephremov, A. (2006). The epidermis-specific extracellular BODYGUARD controls cuticle development and morphogenesis in *Arabidopsis*. *Plant Cell* 18, 321–339.
 36. Schnurr, J., Shockley, J., and Browse, J. (2004). The acyl-CoA synthetase encoded by LACS2 is essential for normal cuticle development in *Arabidopsis*. *Plant Cell* 16, 629–642.
 37. Petit, J., Bres, C., Mauxion, J.P., Tai, F.W.J., Martin, L.B.B., Fich, E.A., Joubès, J., Rose, J.K.C., Domergue, F., and Rothan, C. (2016). The glycerol-3-phosphate acyltransferase GPAT6 from tomato plays a central role in fruit cutin biosynthesis. *Plant Physiol.* 171, 894–913.
 38. Shi, J.X., Adato, A., Alkan, N., He, Y., Lashbrooke, J., Matas, A.J., Meir, S., Malitsky, S., Isaacson, T., Prusky, D., et al. (2013). The tomato SISHINE3 transcription factor regulates fruit cuticle formation and epidermal patterning. *New Phytol.* 197, 468–480.
 39. Philippe, G., Gaillard, C., Petit, J., Geneix, N., Dalgalarrodo, M., Bres, C., Mauxion, J.P., Franke, R., Rothan, C., Schreiber, L., et al. (2016). Ester cross-link profiling of the cutin polymer of wild-type and cutin synthase tomato mutants highlights different mechanisms of polymerization. *Plant Physiol.* 170, 807–820.
 40. Pinot, F., and Beisson, F. (2011). Cytochrome P450 metabolizing fatty acids in plants: characterization and physiological roles. *FEBS J.* 278, 195–205.
 41. Wellesen, K., Durst, F., Pinot, F., Benveniste, I., Nettesheim, K., Wisman, E., Steiner-Lange, S., Saedler, H., and Yephremov, A. (2001). Functional analysis of the LACERATA gene of *Arabidopsis* provides evidence for different roles of fatty acid ω-hydroxylation in development. *Proc. Natl. Acad. Sci. USA* 98, 9694–9699.
 42. Girard, A.L., Mount, F., Lemaire-Chamley, M., Gaillard, C., Elmorjani, K., Vivancos, J., Runavot, J.L., Quemener, B., Petit, J., Germain, V., et al. (2012). Tomato GDSL1 is required for cutin deposition in the fruit cuticle. *Plant Cell* 24, 3119–3134.
 43. Fich, E.A., Segerson, N.A., and Rose, J.K.C. (2016). The plant polyester cutin: biosynthesis, structure, and biological roles. *Annu. Rev. Plant Biol.* 67, 207–233.
 44. Leide, J., Hildebrandt, U., Reussing, K., Riederer, M., and Vogg, G. (2007). The developmental pattern of tomato fruit wax accumulation and its impact on cuticular transpiration barrier properties: effects of a deficiency in a beta-ketoacyl-coenzyme A synthase (LecER6). *Plant Physiol.* 144, 1667–1679.
 45. Giménez, E., Castañeda, L., Pineda, B., Pan, I.L., Moreno, V., Angosto, T., and Lozano, R. (2016). TOMATO AGAMOUS1 and ARLEQUIN/TOMATO AGAMOUS-LIKE1 MADS-box genes have redundant and divergent functions required for tomato reproductive development. *Plant Mol. Biol.* 91, 513–531.
 46. Lashbrooke, J., Adato, A., Lotan, O., Alkan, N., Tsimbalist, T., Rechav, K., Fernandez-Moreno, J.P., Widemann, E., Grausem, B., Pinot, F., et al. (2015). The tomato MIXTA-Like transcription factor coordinates fruit epidermis conical cell development and cuticular lipid biosynthesis and assembly. *Plant Physiol.* 169, 2553–2571.
 47. Martin, L.B.B., Sherwood, R.W., Nicklay, J.J., Yang, Y., Muratore-Schroeder, T.L., Anderson, E.T., Thannhauser, T.W., Rose, J.K.C., and Zhang, S. (2016). Application of wide selected-ion monitoring data-independent acquisition to identify tomato fruit proteins regulated by the CUTIN DEFICIENT2 transcription factor. *Proteomics* 16, 2081–2094.
 48. Nadakuduti, S.S., Pollard, M., Kosma, D.K., Allen, C., Jr., Ohlrogge, J.B., and Barry, C.S. (2012). Pleiotropic phenotypes of the sticky peel mutant provide new insight into the role of CUTIN DEFICIENT2 in epidermal cell function in tomato. *Plant Physiol.* 159, 945–960.
 49. Xiong, C., Xie, Q., Yang, Q., Sun, P., Gao, S., Li, H., Zhang, J., Wang, T., Ye, Z., and Yang, C. (2020). WOOLLY, interacting with MYB transcription factor MYB31, regulates cuticular wax biosynthesis by modulating CER6 expression in tomato. *Plant J.* 103, 323–337.
 50. Wu, M., Zhou, Y., Ma, H., Xu, X., Liu, M., and Deng, W. (2024). SIMYB72 interacts with SITAGL1 to regulate the cuticle formation in tomato fruit. *Plant J.* 120, 1591–1604.
 51. Isaacson, T., Kosma, D.K., Matas, A.J., Buda, G.J., He, Y., Yu, B., Pravitasari, A., Batteas, J.D., Stark, R.E., Jenks, M.A., and Rose, J.K.C. (2009). Cutin deficiency in the tomato fruit cuticle consistently affects resistance to microbial infection and biomechanical properties, but not transpirational water loss. *Plant J.* 60, 363–377.

52. Borisjuk, N., Hrmova, M., and Lopato, S. (2014). Transcriptional regulation of cuticle biosynthesis. *Biotechnol. Adv.* 32, 526–540.
53. González-Valenzuela, L., Renard, J., Depège-Fargeix, N., and Ingram, G. (2023). The plant cuticle. *Curr. Biol.* 33, 210–214.
54. Javelle, M., Vernoud, V., Rogowsky, P.M., and Ingram, G.C. (2011). Epidermis: the formation and functions of a fundamental plant tissue. *New Phytol.* 189, 17–39.
55. Oshima, Y., Shikata, M., Koyama, T., Ohtsubo, N., Mitsuda, N., and Ohme-Takagi, M. (2013). MIXTA-Like transcription factors and WAX INDUCER1/SHINE1 coordinately regulate cuticle development in arabidopsis and *torenia fournieri*. *Plant Cell* 25, 1609–1624.
56. Gao, J., Wang, G., Ma, S., Xie, X., Wu, X., Zhang, X., Wu, Y., Zhao, P., and Xia, Q. (2015). CRISPR/Cas9-mediated targeted mutagenesis in *Nicotiana tabacum*. *Plant Mol. Biol.* 87, 99–110.
57. Liu, Y., Shi, Y., Zhu, N., Zhong, S., Bouzayen, M., and Li, Z. (2020). SIGRAS4 mediates a novel regulatory pathway promoting chilling tolerance in tomato. *Plant Biotechnol. J.* 18, 1620–1633.
58. Huang, H., Burghardt, M., Schuster, A.C., Leide, J., Lara, I., and Riederer, M. (2017). Chemical composition and water permeability of fruit and leaf cuticles of *Olea europaea* L. *J. Agric. Food Chem.* 65, 8790–8797.
59. Su, D., Wen, L., Xiang, W., Shi, Y., Lu, W., Liu, Y., Xian, Z., and Li, Z. (2022). Tomato transcriptional repressor SIBES1.8 influences shoot apical meristem development by inhibiting the DNA binding ability of SIWUS. *Plant J.* 110, 482–498.
60. Chen, H., Zou, Y., Shang, Y., Lin, H., Wang, Y., Cai, R., Tang, X., and Zhou, J.M. (2008). Firefly luciferase complementation imaging assay for protein-protein interactions in plants. *Plant Physiol.* 146, 368–376.
61. Zentella, R., Hu, J., Hsieh, W.P., Matsumoto, P.A., Dawdy, A., Barnhill, B., Oldenhof, H., Hartweck, L.M., Maitra, S., Thomas, S.G., et al. (2016). O-glcNAcylation of master growth repressor DELLA by SECRET AGENT modulates multiple signaling pathways in Arabidopsis. *Genes Dev.* 30, 164–176.

STAR★METHODS

KEY RESOURCES TABLE

REAGENT or RESOURCE	SOURCE	IDENTIFIER
Antibodies		
GFP/eGFP Tag Rabbit pAb	Zen Bioscience	Cat# 300943; RRID: AB_3675496
GFP tag Monoclonal antibody	Proteintech	Cat#66002-1-Ig; RRID: AB_11182611
DYKDDDDK tag Monoclonal antibody	Proteintech	Cat#66008-4-Ig; RRID: AB_2918475
Bacterial and virus strains		
DH5 α Chemically Competent Cell	WEIDI	Cat#DL1001M
BL21 (DE3) pLysS Chemically Competent Cell	WEIDI	Cat#EC1003
GV3101 Chemically Competent Cell	WEIDI	Cat#AC1001L
GV3101 (pSoup) Chemically Competent Cell	WEIDI	Cat#AC1002M
Chemicals, peptides, and recombinant proteins		
Oil red O saturated solution, 0.5%	Solarbio	Cat#G1260
Hygromycin B	Solarbio	Cat#H8080
Glutaraldehyde, 2.5% (EM Grade)	Solarbio	Cat#P1126
IPTG (Isopropyl β -D-Thiogalactopyranoside)	Solarbio	Cat#I8070
Kanamycin sulfate	Genview	Cat#AK177
Heptadecanoic acid methyl ester	ZZSTANDARD	Cat#ZC-59818
Cellulase "Onozuka" R-10	Yakult	Cat#MX7352
Pectolyase Y-23	Yakult	Cat#MX7354
Pyridine	Macklin	Cat#P816289
N, O-Bis (trimethylsilyl) trifluoroacetamide with trimethylchlorosilane	Macklin	Cat#N803298
His-SIGRAS9	This paper	N/A
His-SIZHD17	This paper	N/A
His-SICD2	This paper	N/A
GST-SIMIXTA-like	This paper	N/A
GST-SIMBP3	This paper	N/A
GST-SITAGL1	This paper	N/A
GFP-SIZHD17	This paper	N/A
GFP-SIMBP3	This paper	N/A
FLAG-SIMBP3	This paper	N/A
FLAG-SIMIXTA-like	This paper	N/A
FLAG-SICD2	This paper	N/A
FLAG-SITAGL1	This paper	N/A
Critical commercial assays		
RNAprep Pure Plant Kit	TIANGEN	Cat#DP432
Prime Script TM RT reagent Kit with gDNA Eraser	Takara	Cat#RR047A
TB Green [®] Premix Ex Taq [™] II	Takara	Cat#RR820A
Dual-Luciferase [™] Reporter (DLR [™]) Assay Systems	Promega	Cat#E1910
GST Sep Glutathione Agarose Resin 4FF	Yeasen	Cat#20508ES10
Ni-NTA Agarose	QIAGEN	Cat#30210
Pierce [™] Biotin 3' End DNA Labeling Kit	Thermo Fisher	Cat#89818
Light Shift Chemiluminescent EMSA Kit	Thermo Fisher	Cat#20148
Plant Total Protein Extraction Kit	Sigma	Cat#PE0230
Beaver Beads [®] Protein A (or A/G)	Beaver	Cat#22202
Immunoprecipitation Kit		

(Continued on next page)

Continued

REAGENT or RESOURCE	SOURCE	IDENTIFIER
Deposited data		
Raw RNA-seq data	https://ngdc.cncb.ac.cn/gsa/	GSA Bio Project: PRJCA018221
Experimental models: Organisms/strains		
Tomato (<i>Solanum lycopersicum</i>): <i>Sigras9-CR</i>	This paper	N/A
Tomato (<i>Solanum lycopersicum</i>): <i>SIGRAS9-RNAi</i>	This paper	N/A
Tomato (<i>Solanum lycopersicum</i>): <i>SIZHD17-RNAi</i>	This paper	N/A
Tomato (<i>Solanum lycopersicum</i>): <i>Slmbp3-CR</i>	This paper	N/A
Tomato (<i>Solanum lycopersicum</i>): 35S: <i>SIZHD17/Sigras9-CR</i>	This paper	N/A
Tomato (<i>Solanum lycopersicum</i>): 35S: <i>SIZHD17/SIGRAS9-RNAi</i>	This paper	N/A
Tobacco (<i>Nicotiana benthamiana</i>)	This paper	N/A
Recombinant DNA		
CRISPR/Cas9 SIGRAS9/pORE	This paper	N/A
CRISPR/Cas9 SIMBP3/pAGM4723	This paper	N/A
RNAi SIGRAS9/pCAMBIA 1301	This paper	N/A
RNAi SIZHD17/pCAMBIA 1301	This paper	N/A
Overexpression SIZHD17/pCAMBIA1300	This paper	N/A
pGreenII 62-SK 62SK-SIGRAS9	This paper	N/A
pGreenII 62-SK 62SK-SIZHD17	This paper	N/A
pGreenII 62-SK 62SK-SIMBP3	This paper	N/A
pGreenII 62-SK 62SK-SIMIXTA-like	This paper	N/A
pGreenII 62-SK 62SK-SICD2	This paper	N/A
pGreenII 62-SK 62SK-SITAGL1	This paper	N/A
pGreenII 0800-LUC 0800-SICYP86A69	This paper	N/A
pGreenII 0800-LUC 0800-SICYP77A1	This paper	N/A
pGreenII 0800-LUC 0800-SIGPAT6	This paper	N/A
pGreenII 0800-LUC 0800-SIMBP3	This paper	N/A
pCold™ TF His-SIGRAS9	This paper	N/A
pCold™ TF His-SIZHD17	This paper	N/A
pCold™ TF His-SICD2	This paper	N/A
pCold™-GST GST-SIMBP3	This paper	N/A
pCold™-GST GST-SITAGL1	This paper	N/A
pGEX-4T-1 GST-SIMIXTA-like	This paper	N/A
pCAMBIA-nLUC nLUC-SIGRAS9	This paper	N/A
pCAMBIA-nLUC nLUC-SIZHD17	This paper	N/A
pCAMBIA-cLUC cLUC-SIMBP3	This paper	N/A
pCAMBIA-cLUC cLUC-SIMIXTA-like	This paper	N/A
pCAMBIA-cLUC cLUC-SICD2	This paper	N/A
pCAMBIA-cLUC cLUC-SITAGL1	This paper	N/A
pCAMBIA-cLUC cLUC-SISHIN3	This paper	N/A
pGreen35S-GFP GFP-SIZHD17	This paper	N/A
pGreen35S-GFP GFP-SIMBP3	This paper	N/A
pCAMBIA1301-3×Flag FLAG-SIMBP3	This paper	N/A
pCAMBIA1301-3×Flag FLAG-SITAGL1	This paper	N/A
pCAMBIA1301-3×Flag FLAG-SIMIXTA-like	This paper	N/A
pCAMBIA1301-3×Flag FLAG-SICD2	This paper	N/A
Software and algorithms		
GraphPad prism	GraphPad Software	https://www.graphpad.com
CorelDRAW	Corel Software	https://www.corel.com/en
ImageJ	ImageJ Software	https://imagej.net

EXPERIMENTAL MODEL AND STUDY PARTICIPANT DETAILS

Wild-type tomato (*Solanum lycopersicum* cv. Micro-Tom) and transgenic plants were cultivated in the growth chamber under controlled conditions (16 h: 8 h, 25°C: 18°C, light: dark; 250 mol m⁻² s⁻¹ intense light; 60% relative humidity).

METHOD DETAILS

Generation of plant materials

To generate CRISPR/Cas9 mutant plants, a 20 bp target sequence was cloned into a plant binary vector constructed according to Gao.⁵⁶ *A. tumefaciens*-mediated infection methods were performed to generate transgenic plants in wild-type tomato plants (*Solanum lycopersicum* cv. Micro-Tom) based on Shi.² The different type of genome editing in homozygous mutants were further genotyped by sanger sequencing for subsequent experiments. To generate RNA-interference (RNAi) plants, a 271 bp long sequence fragment of *SIGRAS9* gene and a 259 bp sequence fragment of *SIZHD17* gene were cloned into pCAMBIA1301, a modified plant binary vector under the control of the CaMV35S promoter. All transgenic plants were generated via *A. tumefaciens*-mediated infection method as previously described.⁵⁷ All positive transgenic lines were screened by Kanamycin (100 mg/L) and PCR confirmation, and the relative expression level of *SIGRAS9* and *SIZHD17* were determined by real-time qPCR in homozygous T2 or T3 generations. *SIGRAS9*-RNAi and *SIZHD17*-RNAi lines displaying strong down-regulation as well as *SIGRAS9* knock-out (*Slgras9*-CR), *SIGRAS9*-RNAi, *SIZHD17*-RNAi and *Slmbp3* knock-out (*Slmbp3*-CR) lines have been generated previously^{2,4} and used in the present study. The primers are listed in [Table S2](#).

To generate restorer plants, full length of *SIZHD17* were cloned into pCAMBIA1300-35S, a modified plant binary vector under the control of the CaMV35S promoter. The restorer plants were generated via the *tumefaciens*-mediated infection method as previously described.² All positive transgenic lines were screened by hygromycin (100 mg/L) and PCR confirmation, and the relative expression level of *SIZHD17* were determined by real-time qPCR in leaves. The primers are listed in [Table S2](#).

RNA extraction, cDNA synthesis, real-time qPCR and RNA-seq

Plant tissues were collected at the corresponding stages and frozen in liquid nitrogen, total RNA from the whole fruits of WT, *Slgras9*-CR, *SIZHD17*-RNAi and *Slmbp3*-CR lines at mature green stage were isolated by RNAprep Pure kit (TIANGEN, China). The integrity of total RNA was validated by agarose gel electrophoresis, the concentration was measured by a NanoDrop 1000 (Thermo, USA). Reverse transcribed into cDNA and real-time qPCR were performed using PrimeScript RT reagent Kit with gDNA Eraser (Takara, Japan) and TB Green Premix Ex TaqTM II (Tli RNaseH Plus) (TAKARA, Japan), respectively. The real-time qPCR procedure was conducted on the Bio-Rad CFX96 system (Bio-Rad, USA). The relative fold change of each gene was calculated by 2^{-ΔΔCt} method, and *SlActin* was used as the internal reference gene. The primers are listed in [Table S2](#).

The total RNA of WT, *Slgras9*-CR and *SIZHD17*-RNAi fruits at mature green stage were analyzed by RNA-seq. RNA purification, reverse transcribed into cDNA, library construction and sequencing were carried out in Shanghai Majorbio Bio-pharm Biotechnology Co., Ltd. (Shanghai, China). The expression level of each gene was normalized according to the transcripts per million reads (TPM) method, the gene abundances was quantified by RSEM software. Differentially expressed genes (DEGs) were identified by the DESeq2 R package, DEGs with parameters: log₂ Fold Change ≥ 1.00 and adjusted P-adjust value ≤ 0.01 were considered to be significantly different expressed genes between two different groups.

Fruit pericarp microstructure observation

The data of the force to pierce the exocarp was measured by GY4 digital fruit texture analyzer (Aiwoshi, China) based on the method of Yang.⁶ The GY4 digital fruit texture analyzer is equipped with a circular probe with diameter 7 mm, and the force to pierce the exocarp is recorded in Newton (N). The tomato fruits at mature green and red ripe stages were collected to measure the force to pierce the exocarp, and at least 15 fruits from different plants were measured at each stage.

The pericarp of WT, *SIGRAS9*-RNAi, *Slgras9*-CR, *SIZHD17*-RNAi and *Slmbp3*-CR fruit were fixed to the FAA solution and embedded in paraffin according to the method as previously described.⁶ Eight-micrometer slices of the pericarp from WT, *SIGRAS9*-RNAi, *Slgras9*-CR, *SIZHD17*-RNAi and *Slmbp3*-CR fruit were stained with oil red O (ORO) solution. To further observe the microstructures of the pericarp, the pericarp slices of WT, *SIGRAS9*-RNAi, *Slgras9*-CR, *SIZHD17*-RNAi and *Slmbp3*-CR fruit at mature green and red ripe stage fixed by FAA solution were dehydrated in a series of ethanol solution and then dried by carbon dioxide. TM4000Plus II (Hitachi, Japan) was used to take scanning electron microscope (SEM) images of the pericarp microstructures and fruit surface. The cuticle thickness and cuticle permeation thickness were measured by ImageJ software. The statistics data of cuticle thickness and cuticle permeation thickness come from ten slices of ten fruits. 2-3 positions were selected for each slice to measure the cuticle thickness and cuticle permeation thickness.

For the observation of epidermal cell morphology, the exocarp of WT, *SIGRAS9*-RNAi, *Slgras9*-CR, *SIZHD17*-RNAi and *Slmbp3*-CR fruit at mature green stage were observed by a confocal laser scanning microscopy (Leica, Germany). For cuticle structure observation, the exocarp of WT, *Slgras9*-CR and *SIZHD17*-RNAi fruit were thinly sliced and fixed in glutaraldehyde solution (2.5%). The slices were observed by Tecnai T12 TWIN transmission electron microscope (FEI, USA).

Cutin monomer analyses

The isolated red ripe fruit peel (10 cm^2) was soaked into citric acid buffer containing cellulase (1%) and pectinase (1%) for 7–10 days to remove the exocarp cells on the cuticular membranes according to Huang.⁵⁸ Add 1 mM sodium azide to the citric buffer to avoid microbial growth. Methyl heptadecanoate (1 mg/mL stock) was used as the internal standard. The cuticular membranes were delipidated, depolymerized and analyzed according to the method described by Jenkin.²⁶ Eight discs were taken from the enzymolized fruit peel with a punch, and the discs were soaked in chloroform for 24 h to remove the epidermal wax. Add 3.6 mL methanol, 0.9 mL methyl acetate and 1.5 mL sodium methoxide into each tube. The mixture was reacted at 60°C for 2 h and mix it every 10 min. 10 mL dichloromethane and 1.5 mL glacial acetic acid were added into the mixture, followed by washing with 0.5 M NaCl solution for three times to extract the organic phase. The organic phase was transferred to a new centrifuge tube and dried under nitrogen. Add 100 μL pyridine and 100 μL N, O-Bis(trimethylsilyl) trifluoroacetamide with trimethylchlorosilane (BSTFA) to the dried sample, and the sample was derivatized at 80°C for 1 h. After drying under nitrogen, the sample was redissolved with 1 mL chloroform for GC-MS analysis. Cutin monomer analysis was performed on an Agilent GC-MS instrument (8890-7000E, Agilent) with $30\text{ m} \times 0.25\text{ mm} \times 0.25\text{ }\mu\text{m}$ HP-5 MS column and helium as carrier gas. The GC was performed with temperature-programmed automatic injection at 50°C , holding for 5 min at 50°C , temperature increase to 200°C at a rate of $20^\circ\text{C min}^{-1}$ and temperature increase to 320°C at a rate of 3°C min^{-1} for 15 min.

Shelf-life analysis

To assess the shelf life of fruits, the red ripe (Br+7) fruits were harvested and surface sterilized. All the fruits were stored at room temperature for 40 days. The visual softening and collapse of the fruits were photographed and assessed at 20 and 40 days. At least 20 fruits were collected from different lines for shelf-life analysis.

Botrytis cinerea infection

For *Botrytis cinerea* infection assay, *B. cinerea* (B05.10) was cultured on 1% potato dextrose agar, the conidia were collected and filtered for infecting fruit. Surface sterilized red ripe fruit collected from WT and transgenic lines were sprayed thoroughly with spore suspension (2.5×10^5 spores/mL), and kept at 25°C and high humidity conditions. The observation and photograph of the symptoms were taken after 7 days. The infected fruit tissue was collected for total DNA extraction, and real-time qPCR was performed to quantify the *B. cinerea* growth in WT and transgenic fruit.⁶ The primers are listed in [Table S2](#).

Dual-luciferase assays

To explore the regulatory effects of SIGRAS9, SIZHD17, SIMIXTA-like, SICD2, SITAGL1 and SIMBP3 on target genes, the dual-luciferase assays were performed as described previously.¹ Full length of *SIGRAS9*, *SIZHD17*, *SIMIXTA-like*, *SICD2*, *SITAGL1* and *SIMBP3* coding sequences were cloned and inserted into pGreenII 62-SK vector as the effector constructs, and the promoter fragments of target genes were cloned into pGreenII 0800-LUC vector as the reporter constructs. The reporters and effectors were further transiently co-expressed into 1-month-old tobacco (*Nicotiana benthamiana*) leaves. A commercial double luciferase reporter gene assay system (Promega, USA) was used to detect the fluorescence values of LUC and REN. At least five independent biological replicates were measured for each combination. The primers are listed in [Table S2](#).

Electrophoretic mobility shift assay

The full-length coding sequences of *SIGRAS9*, *SIZHD17* and *SICD2* were cloned into pCold TF (TAKARA, Japan) vector, the full-length coding sequence of *SIMIXTA-like* was cloned into pGEX-4T-1 vector, and the full-length *SITAGL1* and *SIMBP3* coding sequences were cloned into the modified pCold-GST (TAKARA, Japan) vector. BL21 cells (WEIDI, China) were used to generate the His-fusion and GST-fusion proteins. The fusion protein was purified using a His-tagged protein purification kit (QIAGEN, Germany) and a GST-tagged protein purification kit (Yeasten Biotechnology) according to our previous study.^{2,59} The designed probes of target genes were biotin-labeled according to the instructions of Biotin 3' End DNA Labeling Kit (Thermo, USA). Light Shift Chemiluminescent EMSA Kit (Thermo, USA) was used to perform the EMSA assay according to the instructions. The unlabeled probes were used as the competitors for labeled probes, and the GGGGG fragment instead of the predicted binding site in the mutant probes were used to confirm the specific binding. The native and mutated probe sequences of each gene are listed in [Table S2](#).

Firefly luciferase complementation imaging (LCI) assay

The LCI assays were carried out based on the description by Chen.⁶⁰ Full length of *SIGRAS9* and *SIZHD17* coding sequences were cloned and inserted into pCAMBIA-nLUC vector, and full length of *SIMIXTA-like*, *SICD2*, *SITAGL1* and *SIMBP3* coding sequences were cloned and inserted into pCAMBIA-cLUC vector. The recombinant plasmids were subsequently transformed into GV3101 and transiently co-expressed in one-month-old tobacco leaves as previously described.¹ Three days after transfection, 1 mM luciferin (Promega, USA) was sprayed onto the injected tobacco leaves and kept in dark for at least 6 min to quench the fluorescence. The LUC images were captured by the low-light cooled CCD imaging apparatus (Alliance, UK). For each combination, at least six independent tobacco leaves were observed. The primers are listed in [Table S2](#).

Co-immunoprecipitation assays (coIP)

The co-immunoprecipitation assays were carried out based on the description by Zentella.⁶¹ Full length of *S/ZHD17* or *SIMBP3* coding sequences were cloned and inserted into pGreen35S-GFP vector, and full length of *SIMIXTA-like*, *SICD2*, *SITAGL1* and *SIMBP3* coding sequences were cloned and inserted into modified pCAMBIA1301-3×Flag vector. The recombinant plasmids were subsequently transformed into GV3101 and transiently co-expressed in one-month-old tobacco leaves. Total protein was extracted according to the instructions of plant total protein extraction kit (Sigma, USA). Co-immunoprecipitation was performed according to the instructions of BeaverBeads Protein A (or A/G) immunoprecipitation Kit. Total protein extracted from tobacco leaves co-expressed by *S/ZHD17*-pGreen35S-GFP or *SIMBP3*-pGreen35S-GFP and the empty pCAMBIA1301-3×Flag was used as negative control to exclude nonspecific binding. Immunoblotting was conducted using anti-GFP (Zen Bioscience, catalog: 300943; protein-tech, catalog: 66002-1-Ig) and anti-FLAG (proteintech, catalog: 66008-4-Ig) antibodies. The primers are listed in [Table S2](#).

QUANTIFICATION AND STATISTICAL ANALYSIS

Two-tailed Student's t test was used for statistical analysis between two samples. Significant differences are indicated by asterisk (* $p < 0.05$, ** $p < 0.01$, *** $p < 0.001$). Duncan's multiple range test was used for statistical analysis among multiple groups. $p < 0.05$ is defined as indicating statistical significance.